Scientific Research Publishing

Open Journal of Applied Sciences, 2024, 14, 643-659
https://www.scirp.org/journal/ojapps
ISSN Online: 2165-3925
ISSN Print: 2165-3917

Progressive Collapse Resistance of a New Staggered Story Isolated System

Yutong Yang[1], Yuancheng Mi[1], Hong Li[1], Zhongfa Guo[2], Dewen Liu[1*], Weiwei Sun[1], Min Lei[3]

[1]College of Civil Engineering, Southwest Forestry University, Kunming, China
[2]College of Civil Engineering, Rattana Bundit University, Bangkok, Thailand
[3]College of Civil Engineering, Southwest Jiaotong University, Chengdu, China
Email: *civil_liudewen@sina.com

How to cite this paper: Yang, Y.T., Mi, Y.C., Li, H., Guo, Z.F., Liu, D.W., Sun, W.W. and Lei, M. (2024) Progressive Collapse Resistance of a New Staggered Story Isolated System. *Open Journal of Applied Sciences*, **14**, 643-659.
https://doi.org/10.4236/ojapps.2024.143046

Received: February 8, 2024
Accepted: March 18, 2024
Published: March 21, 2024

Abstract

A new staggered isolated system developed from the mid-story isolated system is the new staggered story isolated system. There are not many studies on this structure currently. In this study, an 18-story new staggered story isolated system model is established using SAP2000. The dynamic nonlinear dynamic alternate method is used to analyze the structure against progressive collapse. Results show that the structure has good resistance to progressive collapse, and there is no progressive collapse under each working condition. The progressive collapse does not occur for the case of removing only one vertical structural member of the new staggered of isolated system. The side column has big influence on this isolated structures' progressive collapse; the removal of vertical structural member of the isolation layer has less impact on the structure than the removal of the bottom vertical structural member. After the removing of the member, the internal force of the structure will be redistributed, and the axial force of the adjacent columns will change obviously, showing a trend of "near large and far small".

Keywords

The New Staggered Story Isolated System, Alternative Load Path Method, Collapse Resistance

1. Introduction

A novel isolated structure known as the staggered story isolated system was created based on the mid-story isolated system (see Figure 1). While the isolation story of the traditional mid-story isolated system is located in a specific story of the structure, the isolation story of the new staggered story isolated system

is divided into two parts, with the isolation story of the frame part located in the middle of the structure, forming a similar mid-story isolated system. The core-tube's isolation story exists at the bottom of the tube, producing a base isolated system similar to that. Assuring the integrity of the core-tube is a benefit of the new staggered story isolated system. One of the emblematic structures of the new staggered story isolated system, Baotou's Huafa Xintiandi Project [1], is located in Inner Mongolia, China. Additionally, the Second Phase of Haikou Meilan Airport [2] and the North Terminal of Urumqi International Airport [3] both use the new staggered story isolation system. Using a finite element model, Zhang Yafei *et al.* [4] studied the reaction of a super-tall staggered story isolated system to three different types of ground motions and performed a zonal comparison with the response of the mid-story isolated system. In order to study the nonlinear dynamic time-history response under rare earthquakes, Liu Dewen *et al.* [5] constructed a new staggered tale isolated system taking soil-structure interaction into consideration. A nonlinear finite element model of a new staggered story isolated system was created by Zhang Yafei *et al.* [6] and compared to the mid-story isolated system, the base isolation system, and the aseismic structure.

Progressive collapse resistance is a chain reaction failure that occurs in a relatively small part of the structure but results from a large scale collapse failure that is disproportionate to the initial local failure. In the Code for the Design of Collapse Resistance of Building Structures (T/CECS392: 2021) [7], progressive collapse is defined as damage that begins in a relatively small portion of the structure, which then extends from member to member, and eventually leads to the collapse of a part of the structure or the collapse of the whole structure. The engineering community realized the danger of progressive collapse when the Ronan Point flats in London, UK fell [8]. Using SAP2000 finite element analysis software, Shalva Maijanshvili *et al.* [9] examined the progressive collapse resistance of a nine-story steel frame building. Zhu Mingcheng *et al.* [10] conducted a preliminary qualitative examination of the transverse and longitudinal joint

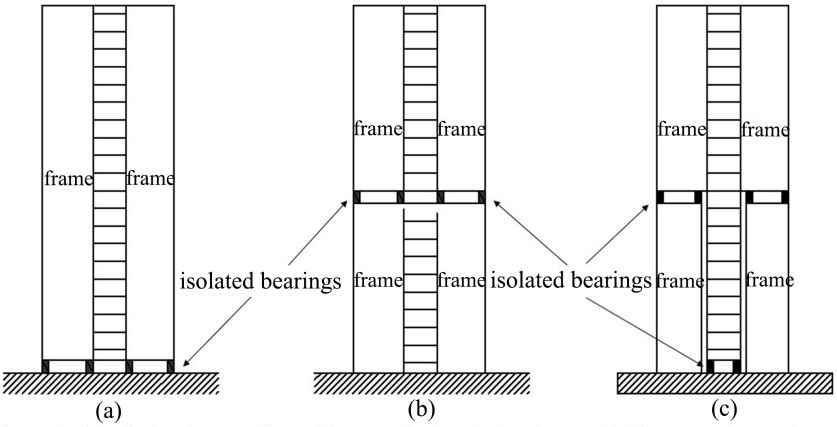

Figure 1. (a) Base isolated structure; (b) Mid-story isolated structure; (c) The new story staggered isolated system.

progressive collapse in north China of a five-story brick and concrete structure caused by a gas explosion. On the basis of the test results and phenomena, Yi Weijian *et al.*, [11] conducted research on the resistance to progressive collapse of reinforced concrete frame buildings, examined the test model frame, and explored the mechanical mechanism of the building. In a finite element simulation investigation of extremely long complex isolated structures, Du Yongfeng *et al.* [12] independently took into account the impact of floor action on the structure's resistance to progressive collapse. Du Yongfeng *et al.* [13] examined a concrete frame isolated structure using LS-DYNA finite element analysis software. The structure's resistance to progressive collapse was assessed by applying explosive loads at various locations in the basement. Zhang Youjia *et al.* [14] established a structural model with finite element software ABAQUS, and analyzed the anti-progressive collapse capability of RC space beam-plate structure under unequal span arrangement by Pushdown method. The research object used by Yu Xiaohui *et al.* [15] was an 8-story, 4-span concrete frame structure, and they compared the pushdown curve under various vertical loading regimes. To determine the collapse resistance mechanism of the structure, Meng Bao *et al.* [16] performed collapse resistance test analysis on frame columns with various joint connection modes.

The previous analyses suggest a scarcity of research on traditional seismic structures, with fewer studies on new staggered-story seismic isolation structures and their ability to withstand continuous collapse. This paper addresses this gap by using SAP2000 to establish an 18-story model of a new staggered-story seismic isolation structure. The study analyses the damage effects of continuous collapse on key components, such as corner and side columns, using the method of removing components. Non-linear dynamic analysis is employed to investigate the continuous collapse resistance, internal forces, and plastic hinge distributions of the remaining members. A comparison is made between the structure's internal forces and plastic hinge distributions before and after the removal of key members to analyze the damage effects of the structure.

2. The Finite Element Model

2.1. Project Overview

A new 18-story staggered story isolated system uses a frame-core tube structure. The building is located in a high-intensity earthquake zone. According to the Chinese code for Seismic Design of Buildings, the site category is Class I, and the seismic fortification intensity is 8 degrees. The basic seismic acceleration is 0.20 g. The construction is a 32 m × 32 m square. The bottom story height is 4.5 m, and the standard story height is 3.6 m. The ninth story's top and the bottom of the core-tube contain the isolation story. The dead load on each story is 3.0 kN/m^2, whereas the live load on each story is 2.0 kN/m^2. The frame beam is meant to have a C30 concrete strength grade, the bottom plate is designed to be 200 mm thick, and the frame column and core-tube are designed to have a C40 concrete strength grade. The frame's beam, column and core tube, have concrete strengths

of C40, 50 mm for protection, HRB400 for the beam and column's reinforcement, and HPB300 for the stirrup. Design calculations were performed on the structure. Table 1 displays the frame beam and column information. They are designed following the Chinese design code and the Code for Design of Concrete Structures and the Code for Seismic Design of Buildings, as shown in Figure 2.

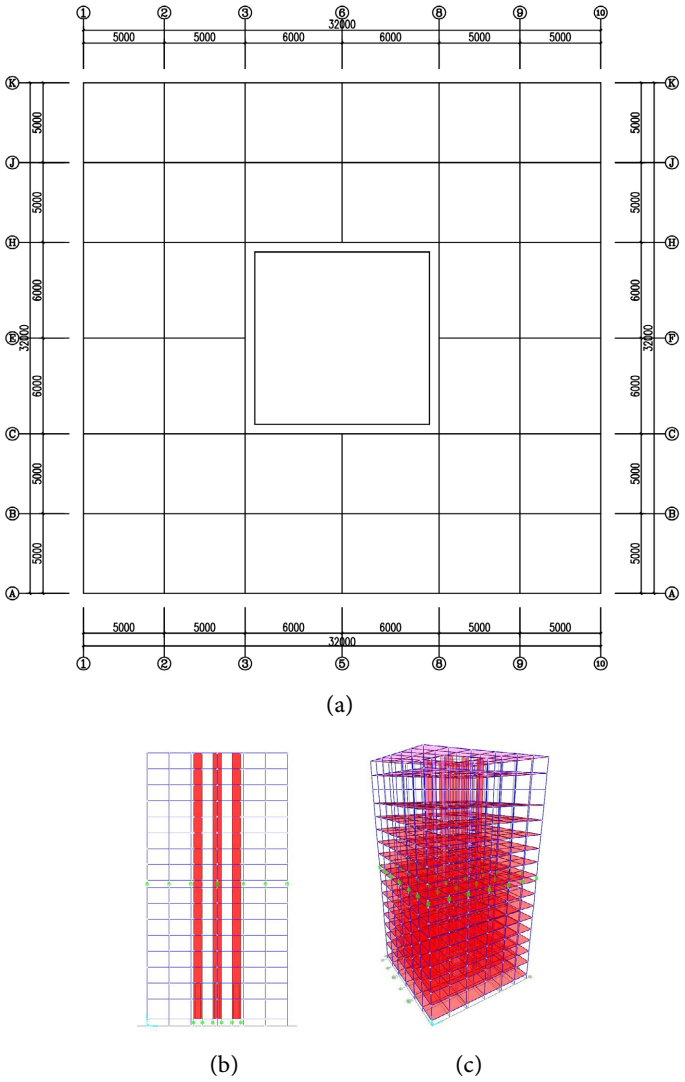

Figure 2. New staggered story isolated structure. (a) Plan; (b) Elevation; (c) 3D.

Table 1. Dimension of frame section.

Component type	Component location/story	Section size/mm	Concrete cover thickness (mm)	Stirrup diameter (mm)	Longitudinal rib size
Frame column	1 - 9	800 × 800	30	10	16C25
	10 - 18	700 × 700	30	10	16C25
Frame beam	1 - 18	700 × 350	50	10	Bottom 4C22 Roof 4C18
Connecting beam	1 - 18	650 × 350	50	10	Bottom 4C22 Roof 4C18

2.2. Model Parameters

The 18 story structure model was created using the finite element program SAP2000. The isolation story is located in the ninth story's top and the bottom of the core tube. The support and column are joined by a solid junction. The structure has 68 isolation supports overall, of which 48 are installed in the frame isolation story and 20 are installed at the base of the core-tube. In each case, LRB600 lead rubber bearings are employed, and important bearing relevant parameters are listed in Table 2. The multi-layer shell is used to imitate the reinforced area at the bottom of the core-tube, while the elastic thin shell is used to simulate the non-reinforced area. Table 3 displays the facts on the shear wall. Takeda hysteresis type was assigned to C40 concrete non-linear materials, whereas Kinematic hysteresis type was assigned to HRB400 steel and HPB300 steel. Frame column adopts PMM plastic hinge and frame beam adopts M3 plastic hinge.

3. Progressive Collapse Resistance Methods

The tie force method, local strengthening, linear static dismantling, linear static alternate path, and nonlinear dynamic alternate path are the basic progressive collapse resistance methods. Among these, the nonlinear dynamic alternate path method is a popular and accurate design method for progressive collapse resistance at the moment [17]. As a result, the nonlinear dynamic alternate path method is employed to evaluate the structure's resistance to collapse.

Table 2. Parameters of isolated bearings.

Type	Effective diameter/mm	Total rubber thickness/mm	Equivalent stiffness		Vertical Stiffness/ ($kN \cdot mm^{-1}$)	Yield force/kN
			100% horizontal shear deformation/ ($kN \cdot m^{-1}$)	250% horizontal shear deformation/ ($kN \cdot m^{-1}$)		
LRB600	600	110	13,110	1580	1580	2800

Table 3. Dimension of frame section.

Section type	Section name	Unit type	Thickness of concrete layer/mm	Reinforcement ratio of vertically distributed reinforcement
Non-bottom reinforcement zone shear wall	Wall	Shell	200	-
Constrained edge member shear wall	Wall-Edge-200	Stratified shell	200	5%
Non-restrained edge member shear wall	Wall-200	Stratified shell	200	0.4%

The nonlinear dynamic method simulates the behavior of a structure under dynamic loading by solving the differential equations of motion of the structure and integrating them directly in a stepwise manner. This method can calculate the internal forces and deformations of the members by solving the differential equations of motion. This method considers the deformation of the structure in both the elastic and plastic ranges, making it more appropriate for structures with nonlinear behavior.

Since the structure in this paper is a new staggered story isolated system, frame columns and isolation of typical parts are selected from the bottom, frame isolation story and core-tube bottom isolation story, and the core-tube shear wall is dismantled component analysis. In accordance with DoD2010 [18] code, when doing a nonlinear dynamic analysis, the structure should first reach a stable state under gravity conditions, and then the target member should be removed sudden until the structure becomes stable or collapses.

The DoD2010 guidelines for collapse say that a structure will enter the state of collapse if the vertical displacement of the removed member's vertex exceeds 20% of the smallest span of the connecting beams. Alternately, use the maximum permissible plastic hinge angle as the criteria for failure. **Figure 3** in the SAP2000 finite element analysis program depicts the five-pointed skeleton curve of the member's plastic hinges. Point A denotes the initial loading, Point B the member yield point, Point C the maximum bearing capacity of the hinges, Point D the remaining strength of the hinges, and Point E the total failure of the hinges. Points IO, LS, and CP, which stand for immediate occupancy, life safety, and collapse prevention, respectively, are acceptable standards for hinge among them. In structural analysis, the member is deemed broken when the plastic hinge of a beam or column structure reaches the CP stage.

The corner column, side column, and inner column, respectively, are the ground floor removal members. From the isolation story of the frame, the corner isolation support, side isolation support, and inner isolation support are each removed in turn. In turn, the Q1 wall, Q2 wall, and Q3 wall support for the core-tube's bottom are removed. According to DoD2010, when removing core-tube shear walls, two times the height of H may be removed for any wall

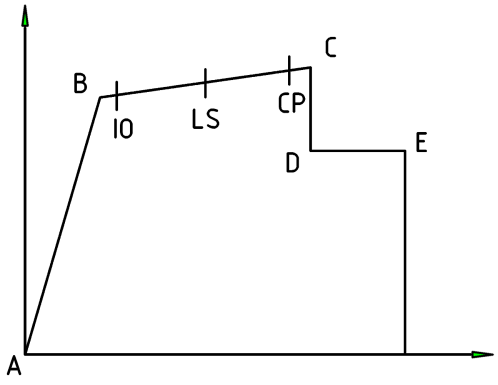

Figure 3. Skeleton curve of plastic hinges.

that is longer than 2H; if the wall is shorter than 2H, the full length may be removed. The walls Q1, Q2, and Q3 were therefore removed for the analysis of progressive collapse resistance. Figure 4 depict the numbers of removed members and columns at the bottom floor as well as the number of removed members and structural supports at the frame's isolation story. The shear wall of the core-tube and the support under the wall are removed, as shown in Figure 5. Remove each member as a working condition, each working condition is shown in Table 4.

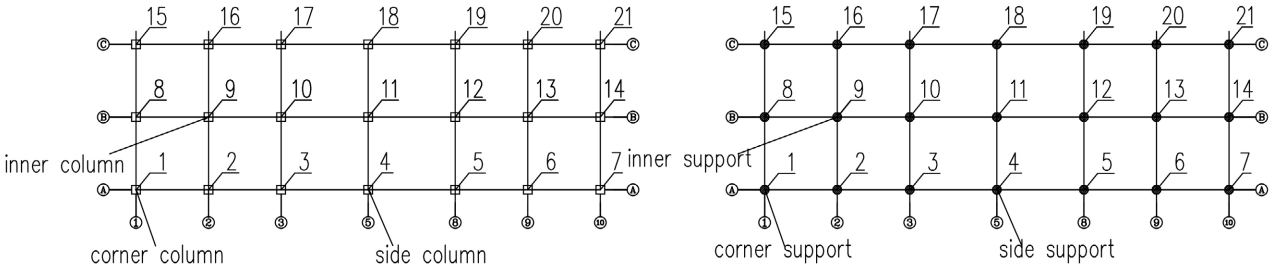

Figure 4. Remove the member diagram.

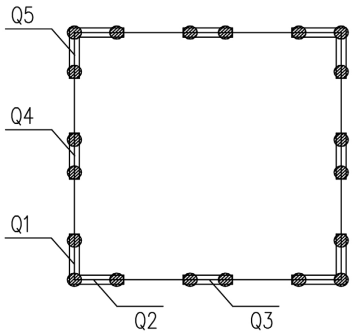

Figure 5. Remove the shear wall of core-tube.

Table 4. Remove the member under different working conditions.

	Remove the member		Remove the member
First working conditions	Remove the ground floor corner column.	eighth working conditions	Remove the support under Q1, Q2 and Q3 walls.
Second working conditions	Remove the ground floor side column.	ninth working conditions	Remove the support under Q1, Q2, Q3 and Q4 walls.
Third working conditions	Remove the ground floor inner column.	tenth working conditions	Remove the support under Q1, Q4 and Q5 walls.
Fourth working conditions	Remove the corner support of the frame isolation story.	Eleventh working conditions	Remove the Q1 wall.
Fifth working conditions	Remove the side support of the frame isolation story.	twelfth working conditions	Remove the Q2 wall.
Sixth working conditions	Remove the inner support of the frame isolation story.	thirteenth working conditions	Remove the Q1, Q2, Q3 and Q4 wall.
seventh working conditions	Remove the support under Q1 and Q2 walls.	fourteenth working conditions	Remove the Q1, Q4 and Q5 wall.

4. Nonlinear Dynamic Analysis of Peripheral Frame Failure

4.1. Analysis of Vertex Displacement-Time History Curve of Remove the Member under Different Working Conditions

The ground floor's vertical displacement-time history responses curve is depicted in Figure 6, and the member of the frame's isolation story's vertical displacement-time history responses curve is depicted in Figure 7. The vertical displacement-time history responses curve demonstrates that after the member is removed, the displacement increases quickly, oscillates up and down over a period of time, and then tends to stabilize. When the side column is removed, the maximum vertex displacement is 22.07 mm, which is 1.83 times greater than the maximum vertex displacement when the ground floor corner column and 1.72 times greater than the maximum vertex displacement when the ground floor inner column are removed. When the isolation support of the frame isolation story is removed, the vertex displacement reaches the maximum when the side support is removed. When the side column is removed, the maximum displacement is 20.48 mm, which is 1.51 times greater than the maximum displacement of the corner support's vertex and 1.52 times greater than the displacement of the interior support's vertex. The maximum vertex displacement is much less than the critical amount for progressive collapse, according to the DoD2010 Code for collapse. When a separate member is removed from the same floor, the corner member's vertex displacement is smaller than that of the inner member and smaller than that of the edge span member. The vertex displacement of the ground floor member is greater than the vertex displacement of the isolation support in the isolation story for the removal of a member at the same position in a different story. The ground floor corner column's, side column's, and inner

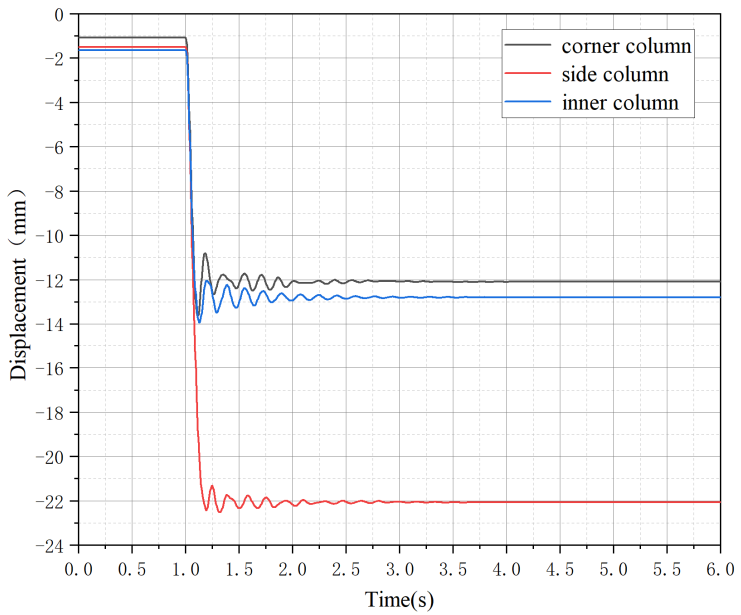

Figure 6. Remove the shear wall of core-tube Vertical displacement of the joint at the top of the removed column on ground floor.

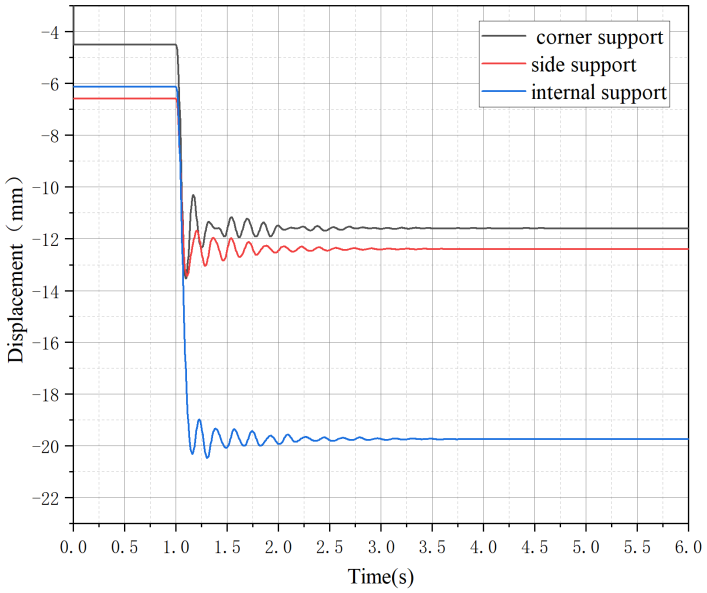

Figure 7. Vertical displacement of the joint at the top of the removed column on frame the top of the removed column on frame.

column's maximum displacements are, respectively, 1.1 times, 1.03 times, and 1.01 times that of the isolation story's equivalent support vertex. After the isolation support of the isolation story is removed, it can be inferred that the remaining structure can sustain more weight.

4.2. Internal Force Analysis of Adjacent Beams under Different Working Conditions

Figure 8 displays the bending moment-time history curves of adjacent frame beams following the removal of members in various working conditions. The moment of the beam end grows quickly in each working conditions when the frame beams are next to each other in the X and Y directions, then oscillates up and down for a period of time before tending to stabilize. The bending moment oscillation interval is larger and the bending moment is less after stability in the first and fourth working conditions. The bending moment oscillation interval is minimal, but the bending moment after stability is significant, in the second and fifth working conditions. The distribution diagram of the structural plastic hinge is shown in **Figure 9**. In each working conditions, the plastic hinge of the frame beam is quickly formed and developed. The most plastic hinges are made in working condition two, and the plastic hinges of neighboring frame beams are generated quickly and rise quickly. The two span frame beams in the center of the frame quickly transition into the plastic stage and form plastic hinges. The moment of the beam end carries the structural resistance, and the structure is in the plastic stage. The frame columns supporting the frame beams in the X and Y directions limit the frame beams' ability to bend once the structure enters the plastic stage, preventing the structure from moving into the suspension cable stage.

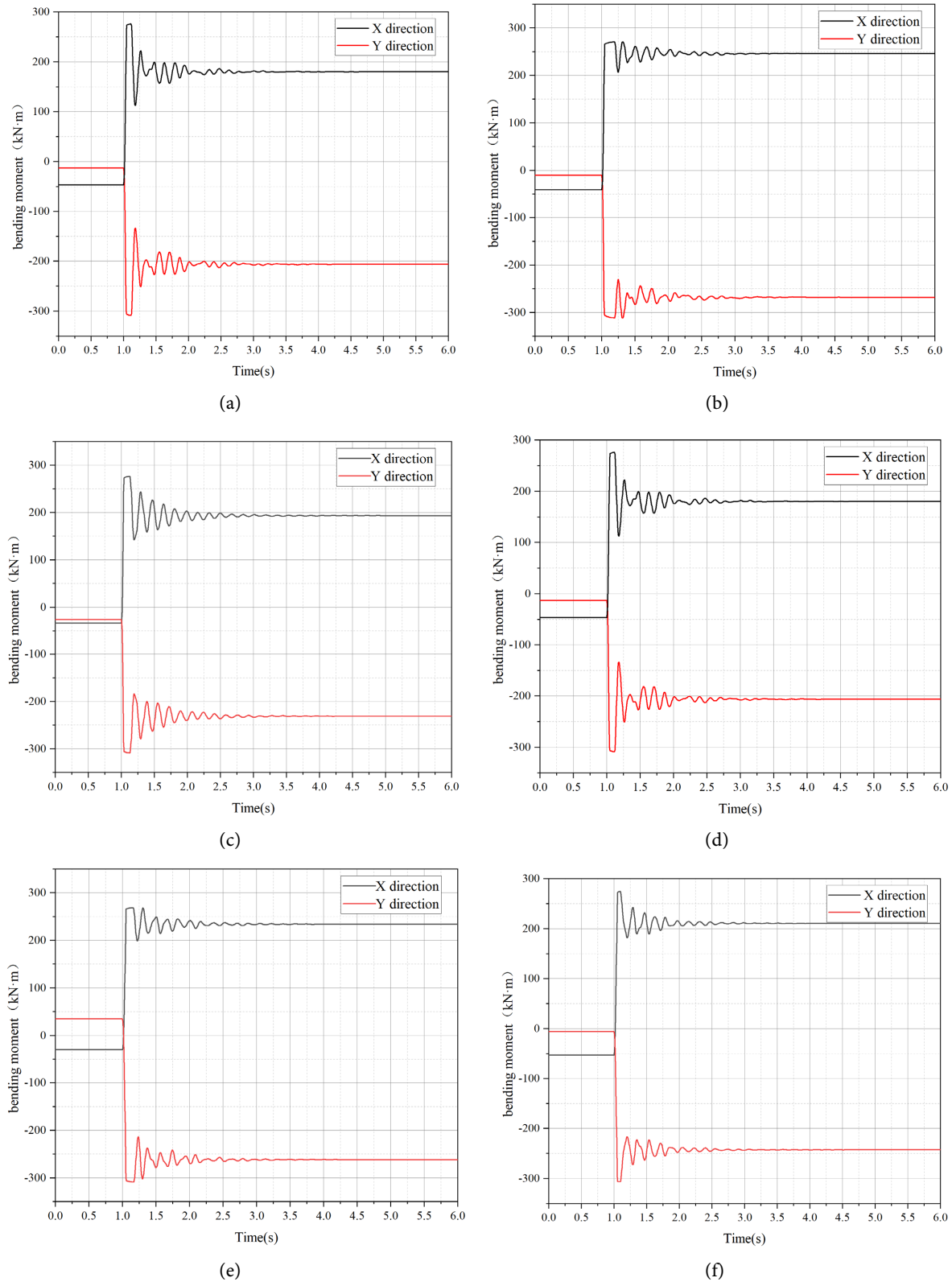

Figure 8. The bending moment-time history curves under each working mode. (a) Bending moment-time history curves of corner column; (b) Bending moment-time history curves of side column; (c) Bending moment-time history curves of inner column; (d) Bending moment-time history curves of corner support; (e) Bending moment-time history curves of side support; (f) Bending moment-time history curves of inner support.

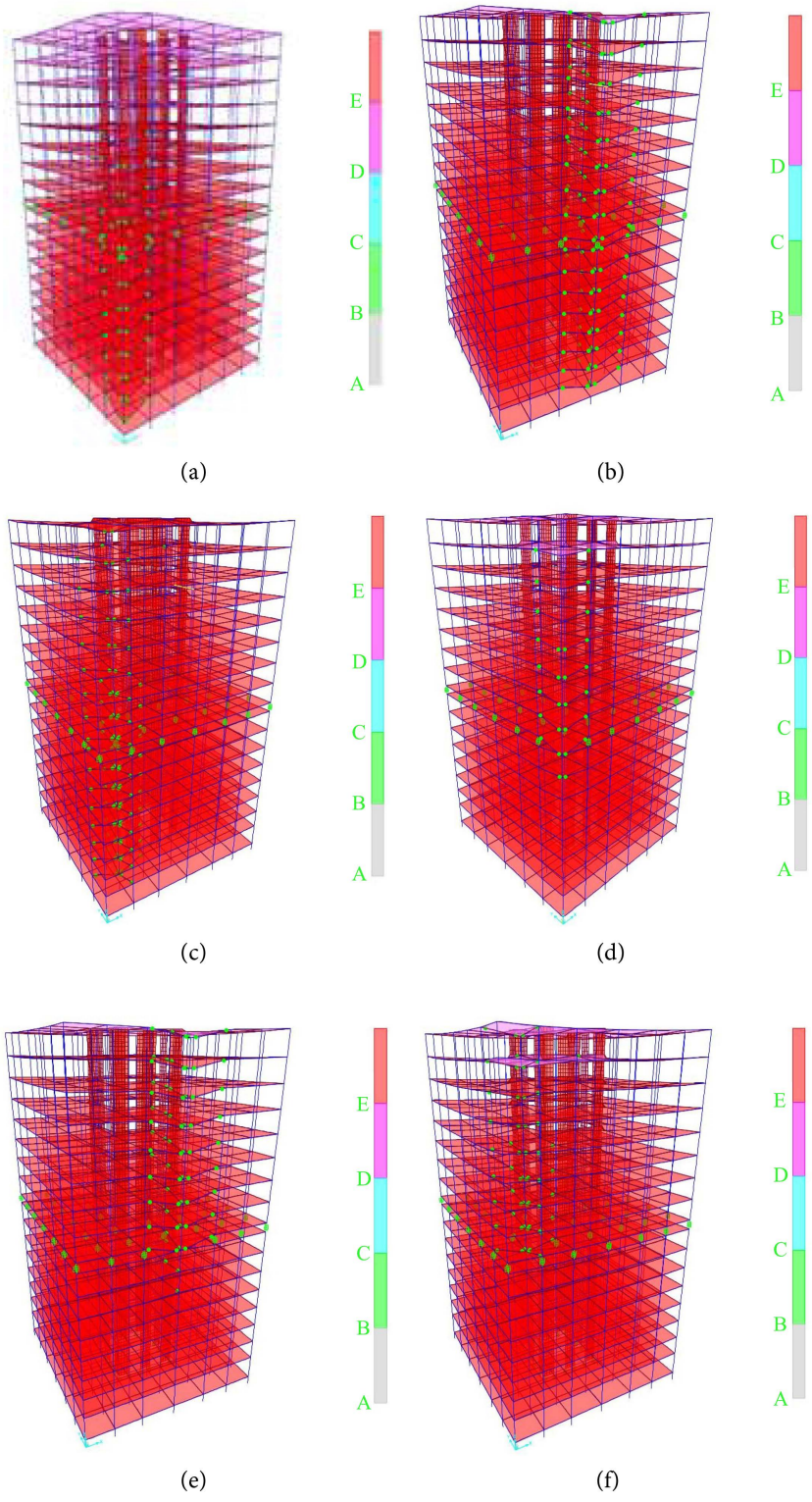

Figure 9. Structure plastic hinge distribution after removal of under each working conditions. (a) Structure plastic hinge distribution after removal of corner column; (b) Structure plastic hinge distribution after removal of side column; (c) Structure plastic hinge distribution after removal of inner column; (d) Structure plastic hinge distribution after removal of corner support; (e) Structure plastic hinge distribution after removal of side support; (f) Structure plastic hinge distribution after removal of inner support.

4.3. Internal Force Analysis of Adjacent Frame Columns under Different Working Conditions

The axial force-time history curves of adjacent columns under working conditions 1, 2, 3, 4, 5, and 6 are displayed in Figure 10 after the members have been removed. The axial force of column No. 2 next to the corner column increases most noticeably in the first working condition when compared to the gravity working condition. The remaining columns' axle forces rise by less than 15% when the front axle force is removed. The axial force of No. 5 column grew by 29%, that of No. 11 column next to the middle column of the side span increased by 36%, and that of the other supports increased by less than 15% in the second operating condition. In the third working mode, the axial force of the No.2 column adjacent to the dismantled column increases by 30%, 27%, 22%, 17%, 16% and 6% respectively, compared with that before the removal of the No. 10 column, No. 1 column, and No. 3, 7 and 11 columns. The axial force growth of the other supports is less than 10% in the fourth operating mode, but it grows by 50% for No. 2 support next to the angular support and by 14% for No. 9 support as compared to prior removal. The axial force of nearby bearing 11 grows by 46% under operating condition five, that of supporting 5 by 31%, and that of other supports is less than 15%. The axial force of nearby supporting 16 increases by 31% under operating condition six mode, that of bearing 2 increases by 29%, and that of other supports is less than 15%.

The findings indicate that the neighboring member is primarily responsible for bearing the axial force of the dismantled member, whereas the other members are only partially responsible. The axial force increase of the neighboring frame column and support is the biggest, which will become the high incidence area of later failure. The force transfer mechanism after the removal of the member gradually weakens as it is far away from the member the impact of an accidental load on a failure member decreases with the distance of the column or frame from the failure member.

5. Nonlinear Dynamic Analysis of Core-Tube Failure

Figure 11 depicts the stress nephogram of the core-tube under various working conditions after the bottom support of the core-tube has been removed. The shear wall's maximum stress in the seventh working condition is 8.1 - 9 Mpa. The shear wall's maximum stress in the ninth working state ranges from 6.3 to 7.2 Mpa. The shear wall is under a maximum stress of 7.65 to 8.5 Mpa in working condition 9. The shear wall's maximum stress in the tenth working state is 15.3 - 17 Mpa. The shear wall's stress exceeds the norm for its strength under maximum stress, and no shear wall is harmed.

After the removal of the shear walls, Figure 12 depicts the stress nephogram of the core-tube. When a wall is removed, the load on the remaining shear walls does not achieve the expected level of strength, resulting in damage to every shear wall. There is barely any structural distortion. The ninth working condition's maximum vertex movement is less than 7 mm. The analysis's findings

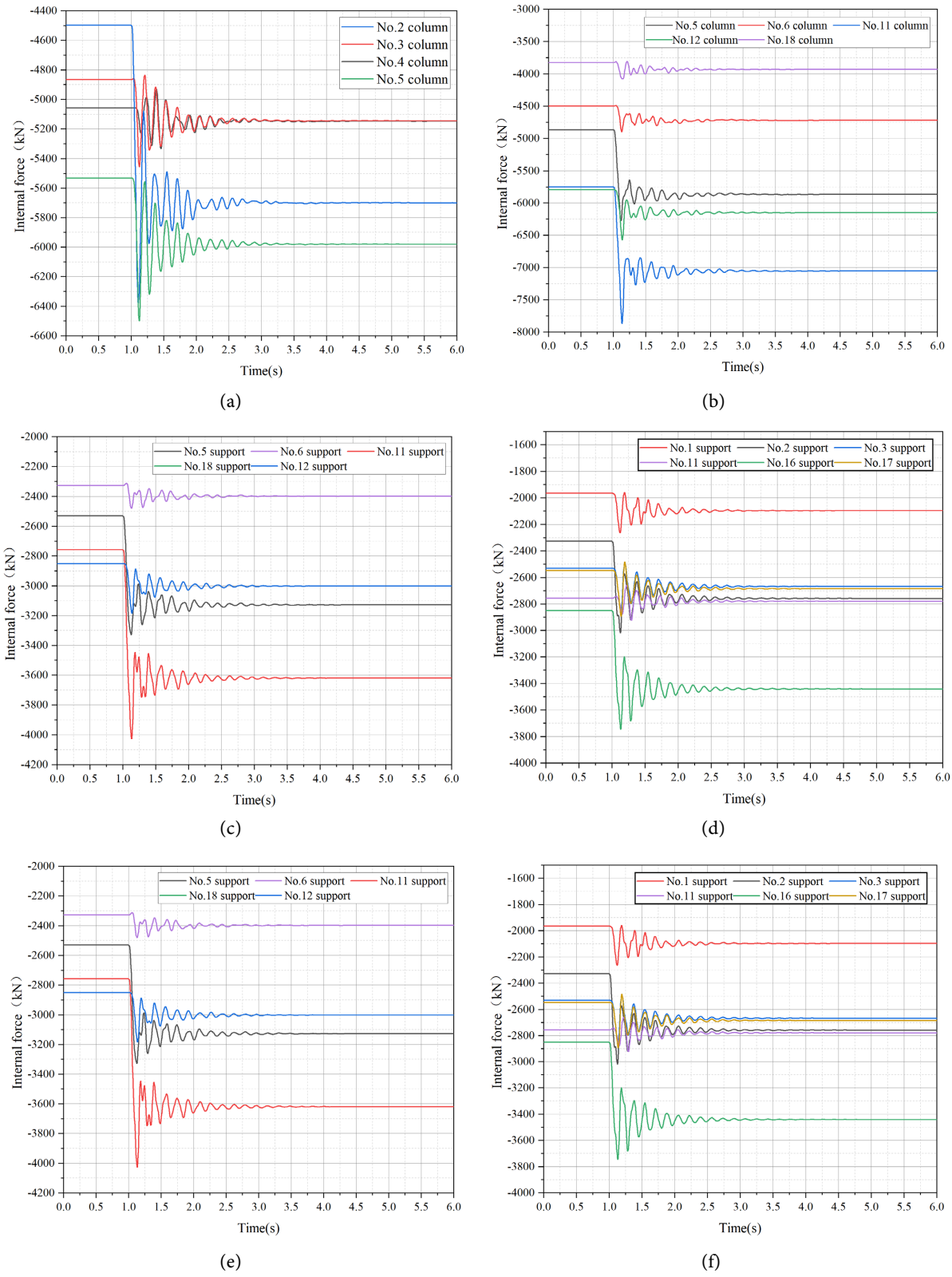

Figure 10. Structure plastic hinge distribution after removal of under each working conditions. (a) Axial force-time history curves of corner column; (b) Axial force-time history curves of side column; (c) Axial force-time history curves of inner column; (d) Axial force-time history curves of corner support; (e) Axial force-time history curves of side support; (f) Axial force-time history curves of inner support.

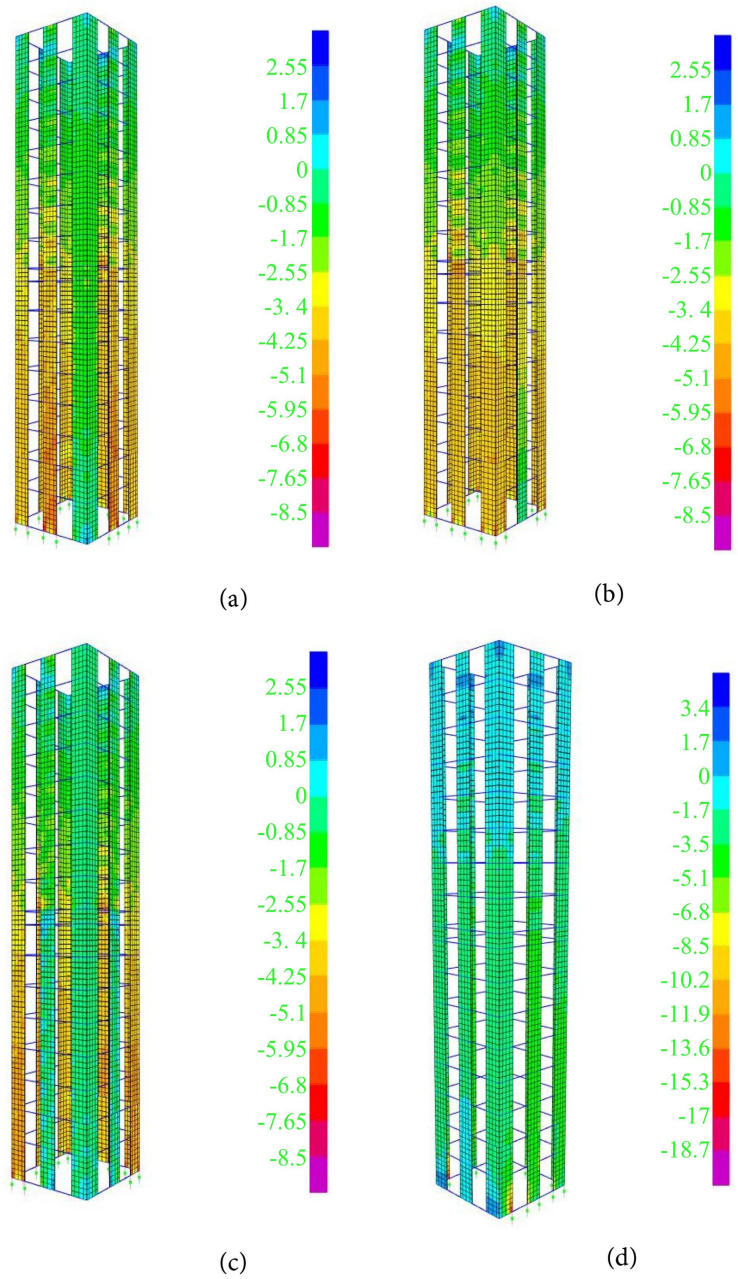

Figure 11. The stress nephogram of the core-tube under various working conditions of the support is removed (Units: Mpa). (a) Remove the stress nephogram of support under Q1 and Q2 shear walls; (b) Remove the stress nephogram of support under Q3 shear walls; (c) Remove the stress nephogram of support under Q1, Q2, Q3 and Q4 shear walls; (d) Remove the stress nephogram of support under Q1, Q4 and Q5 shear walls.

indicate that under any working condition, the residual shear wall can disperse the uneven gravity force and further prevent the progressive collapse of the shear wall In conclusion, the structural deflection is greatly reduced and the vertex displacement is much smaller after the removal of shear walls than it is after the removal of the outer frame columns. Shear walls are strong enough to withstand a building's progressive collapse.

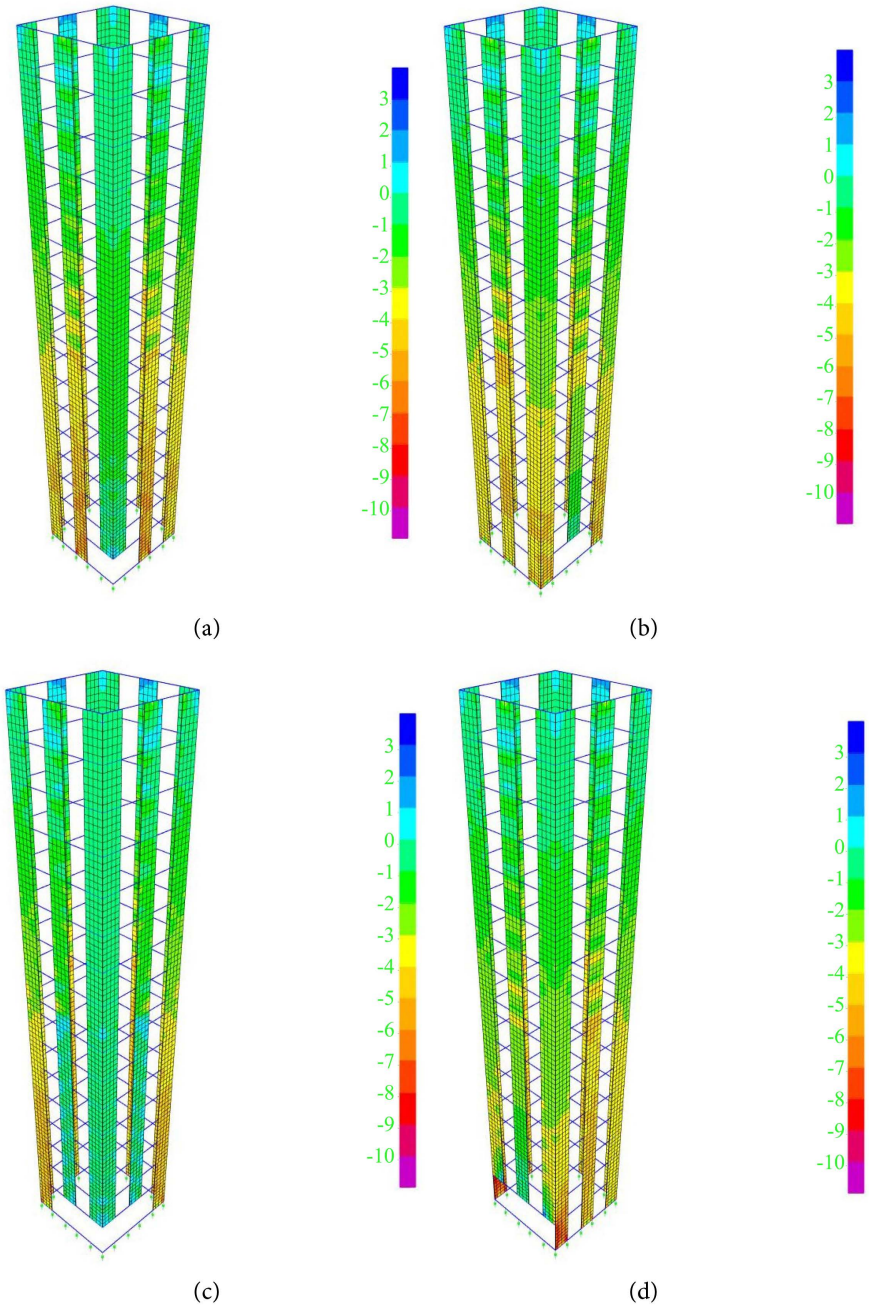

Figure 12. Stress nephogram of core-tube under different wall removal working conditions (Units: Mpa). (a) Remove the stress nephogram of Q1 and Q2 shear walls; (b) Remove the stress nephogram of Q3 shear walls; (c) Remove the stress nephogram of Q1, Q2, and Q4 shear walls; (d) Remove the stress nephogram of Q1, Q4 and Q5 shear walls.

6. Conclusions

A new staggered story isolated system's finite element model is established in this work. The nonlinear dynamic AP method is used to analyze the structure's progressive collapse, and the findings are as follows:

1) No progressive collapse happens under any working condition due to the new staggered story isolated system's strong resistance to it. The progressive

collapse of the structure is the least after the removal of the ground floor corner column and the most after the removal of the ground floor side span column.

2) The failure of the shear wall of the core-tube has little influence on the structure, and the existence of the core-tube can improve the progressive collapse resistance of the structure.

3) The collapse resistance of the remaining structure after the removal of the ground floor members is smaller than that of the remaining structure after the isolation story members.

4) When a member is removed, the neighboring member mostly bears the demolished member's axial force. The axial force decreases with increasing distance from the member, following the trend of "greater near and smaller far". There will be a significant risk of further damage to nearby locations.

Acknowledgements

The writers gratefully acknowledge the financial support of National Natural Science Fund of China (No.52168072 & No.51808467), High-level Talent Support Project of Yunnan Province, China (2020).

Conflicts of Interest

The authors declare no conflicts of interest regarding the publication of this paper.

References

[1] Zhang, H., Li, F., Tai, J., *et al.* (2021) Research on Structural Design of an Isolated High-Rise Building with Enlarged Base and Multiple Tower Story in High-Intensity Area. *Mathematical Problems in Engineering,* **2021**, Article ID: 6669388. https://doi.org/10.1155/2021/6669388

[2] Bu Longgui, Wu Zhongqun, Shu Weinong, *et al.* (2018) Study on Cross-Layer Isolation Design on T2 Terminal of Haikou Meilan International Airport. *Building Structure*, **48**, 79-82.

[3] Shu, W., Zhu, Z., Bu, L., *et al.* (2019) Research and Application of Seismic Isolation Design of Airport Terminal Structure. *Building Structure*, **49**, 5-12.

[4] Zhang, Y., Liu, D., Fang, S., *et al.* (2018) Study on Seismic Response of Super High-Rise Staggered Story Isolation System. *Journal of Building Structures*, **48**, 79-82.

[5] Liu, D., Li, L., Zhang, Y., *et al.* (2022) Study on Seismic Response of a New Staggered Story Isolated Structure Considering SSI Effect. *Journal of Civil Engineering and Management*, **28**, 397-407. https://doi.org/10.3846/jcem.2022.16825

[6] Zhang, Y., Liu, D., Fang, S., *et al.* (2022) Study on Shock Absorption Performance and Damage of a New Staggered Story Isolated System. *Advances in Structural Engineering*, **25**, 1136-1147. https://doi.org/10.1177/13694332211056113

[7] Code for the Design of Collapse Resistance of Building Structures: T/CECS 392: 2021. China Planning Press, Beijing.

[8] Pearson, C. and Delatte, N. (2005) Ronan Point Apartment Tower Collapse and Its Effect on Building Codes. *Journal of Performance of Constructed Facilities*, **19**, 172-177. https://doi.org/10.1061/(ASCE)0887-3828(2005)19:2(172)

[9] Smilowitz, R. and Tennant, D. (2001) Multi-Hazard Design to Resist Progressive Collapse. *Structures*, **109**, 74. https://doi.org/10.1061/40558(2001)74

[10] Zhu, M. and Liu, X. (1994) Analysis of Progressive Collapse of Multi-Story Brick and Concrete Buildings. *Sichuan Building Science Research*, No. 2, 2-5+28.

[11] Yi, W., He, Q. and Xiao, Y. (2007) Collapse Performance of RC Frame Structure. *Journal of Building Structures*, No. 5, 104-109+117.

[12] Du, Y., Zhu, X., Lu, X., *et al.* (2016) Analysis on Progressive Collapse Resistance of Long Complicated Isolated Structures. *Journal of Building Structures*, **49**, 90-95.

[13] Du, Y. and Zeng, X. (2019) Simulation of Uninterrupted Collapse Isolated Structure under Blast Load in Basement. *Journal of Lanzhou University of Technology*, **45**, 113-120.

[14] Zhang, Y.J., Wang, C. and Du, K. (2022) Numerical Study on the Vertical Collapse Capacity of Spatial Beam-Slab Structures with Unequal Spans. *Engineering Mechanics*, **39**, 139-150.

[15] Yu, X., Qian, K. and Lv, D. (2015) Effects of Vertical Loading Patterns on Push-down Analysis of Structures in Resisting Progressive Collapse. *Journal of Building Structures*, **36**, 126-130.

[16] Meng, B., Zhong, W. and Hao, J. (2018) Experimental Study on Anti-Collapse Performance for Beam-to-Column Assemblies of Steel Frame Based on Joint. *Engineering Mechanics*, **35**, 88-96.

[17] Lu, X., Li, Y. and Ye, L. (2011) Theory and Design Method for Progressive Collapse Prevention of Concrete Structures. China Architecture & Building Press, Beijing.

[18] Department of Defense (2010) Unified Facilities Criteria (UFC): Design of Structures to Resist Progressive Collapse. United States Department of Defense, Washington DC.